Remote Sensing of Environment 156 (2015) 561–569

Contents lists available at ScienceDirect

Remote Sensing of Environment

journal homepage: www.elsevier.com/locate/rse

Near-coastal circum-Antarctic iceberg size distributions determined from Synthetic Aperture Radar images

Christine Wesche *, Wolfgang Dierking

Alfred-Wegener-Institut Helmholtz Zentrum für Polar- und Meeresforschung, Bussestrasse 24, 27570 Bremerhaven, Germany

ARTICLE INFO

Article history:
Received 3 September 2014
Received in revised form 28 October 2014
Accepted 30 October 2014
Available online 22 November 2014

Keywords:
Icebergs
SAR
Iceberg mass
Southern Ocean

ABSTRACT

The Radarsat-1 Antarctic Mapping Project (RAMP) compiled a mosaic of Antarctica and the adjacent ocean zone from more than 3000 high-resolution Synthetic Aperture Radar (SAR) images acquired in September and October 1997. The mosaic with a pixel size of 100 m was used to determine iceberg size distributions around Antarctica, combining an automated detection with a visual control of all icebergs larger than 5 km^2 and correction of recognized false detections. For icebergs below 5 km^2 in size, the numbers of false detections and accuracies of size retrievals were analyzed for three test sites. Nearly 7000 icebergs with horizontal areas between 0.3 and 4717.7 km^2 were identified in a near-coastal zone of varying width between 20 and 300 km. The spatial distributions of icebergs around Antarctica were calculated for zonal segments of 20° angular width and related to the types of the calving fronts in the respective section. Results reveal that regional variations of the size distributions cannot be neglected. The highest ice mass accumulations were found at positions of giant icebergs (>18.5 km) but also in front of ice shelves from which larger numbers of smaller icebergs calve almost continuously. Although the coastal oceanic zone covered by RAMP is too narrow compared to the spatial coverage needed for oceanographic research, this study nevertheless demonstrates the usefulness of SAR images for iceberg research and the need for repeated data acquisitions extending ocean-wards over distances of 500 km and more from the coast to monitor iceberg melt and disintegration and the related freshwater input into the ocean.

1. Introduction

The continental margins of Antarctica are surrounded by a large number of ice shelves and glacier tongues, which are the birthplaces of icebergs. Besides basal melting of ice shelves, iceberg calving accounts for a major part of the loss of Antarctica's ice mass (Depoorter et al., 2013). The mass loss can be estimated from calving fluxes and grounding-line fluxes. As icebergs are free-floating pieces of freshwater ice, their drift and decay have an impact on the hydrology, circulation, and biology of the Southern Ocean (Schodlok, Hellmer, Rohardt, and Fahrbach, 2006). For realistic simulations of the ocean dynamics, modelers need to know the numbers and size distributions of icebergs as a function of time and location. Gladstone, Bigg, and Nicholls (2001), e.g., used an iceberg size distribution ranging from 60 to 2200 m for all calving sites to model the freshwater input into the Southern Ocean, based on the assumption that the spatial variation of the iceberg size distributions can be neglected near the Antarctic coastline. Wesche, Jansen, and Dierking (2013), however, showed that the size of icebergs at the timing of calving depends on the surface structure of the respective ice shelf (more specifically on the distance between its surface structures such as crevasses, rifts and pressure ridges) as well as on the width of the calving front. This indicates that the spatial variation of iceberg size distributions around Antarctica may have to be considered in modeling ocean, sea ice, and iceberg dynamics. The objective of this work was to identify icebergs in high-resolution Synthetic Aperture Radar (SAR) images covering the entire coastline of Antarctica and to determine their regional size distributions.

In the last three decades, several studies were published presenting Antarctic iceberg distributions using ship observations (e.g. Orheim (1985), Orheim (1988), Jacka and Giles (2007), Romanov, Romanova, and Romanov (2012)) and satellite altimetry (Tournadre, Girard-Ardhuin, & Legresy, 2012). Huge Antarctic icebergs (>10 nautical miles) were systematically observed by the Brigham Young University (BYU) and the National Ice Center (NIC) using spaceborne scatterometer instruments (Stuart and Long, 2011).

The analysis of SAR imagery fills the gap between ship-borne observations and the detection of giant icebergs by BYU and NIC. By employing high-resolution SAR imagery it is possible to monitor icebergs with lengths between about 100 m and up to several kilometers independent of the cloud cover and light conditions. Until now, SAR images were only used for regional iceberg detections (e.g. Young, Turner, Hyland, and Williams (1998), Gladstone and Bigg (2002)). Through the Radarsat-1 Antarctic Mapping Project (RAMP), radar images covering

---

* Corresponding author at: Alfred-Wegener-Institut Helmholtz Zentrum fuer Polar- und Meeresforschung, Bussestrasse 24, 27570 Bremerhaven, Germany. Tel.: +49 471 4831 1870.
E-mail addresses: christine.wesche@awi.de (C. Wesche), wolfgang.dierking@awi.de (W. Dierking).

http://dx.doi.org/10.1016/j.rse.2014.10.025
0034-4257/

the entire Antarctic continent and adjacent ocean regions are available. They were acquired within 1.5 months during the Antarctic Mapping Mission-1 in 1997 (AMM-1 — Jezek, Sohn, and Noltimier (1998)). This dataset offers the unique opportunity to retrieve local iceberg size distributions, also including smaller icebergs. It has to be noted, though, that each image used for generating the mosaic is a snapshot of iceberg sizes at a particular time.

This paper briefly describes the dataset and the method used for iceberg detection. Based on the results of the detection procedure we present iceberg numbers and size distributions for different coastal regions around the Antarctic continent. We discuss limitations of the RAMP mosaic as well as potential error sources of the iceberg detection. Finally we estimate the near-coastal distribution of ice mass and discuss the need to acquire data over a larger extent from the coast for studying the link between freshwater input into the ocean and iceberg melt and disintegration.

2. Data and method

2.1. Dataset

We based our investigation on the radar image mosaic of the RAMP AMM-1. The mosaic consists of more than 3000 Synthetic Aperture Radar (SAR) images acquired between September and October 1997 at a pixel size of 25 m (Jezek et al., 1998). We used the mosaic at a pixel size of 100 m to reduce the effect of speckle. Hence it was possible to detect icebergs with edge length of only a few hundreds of meters. Additional to the mosaic of the radar intensity images (backscattering coefficients) the respective radar incidence angles were available (http://bprc.osu.edu/rsl/radarsat/data/ — last access 28.10.2014).

Using the RAMP AMM-1 coastline, the area of the continental ice was masked in the images, leaving only the near-coastal ocean regions for further analysis. The minimum width of the imaged ocean zone is 20 km (e.g. Ronne Ice Shelf) and the maximum width at the tip of the Antarctic Peninsula is more than 300 km (Fig. 1).

2.2. Detection of icebergs in the SAR images

We applied an automated iceberg detection method proposed by Wesche and Dierking (2012) on the ocean zone of the RAMP AMM-1-mosaic. The detection method is based on the radar intensity contrast between icebergs and their surroundings (either sea ice or open water). For a brief introduction we start with an overview of the general differences in the radar signatures of icebergs, sea ice and open water.

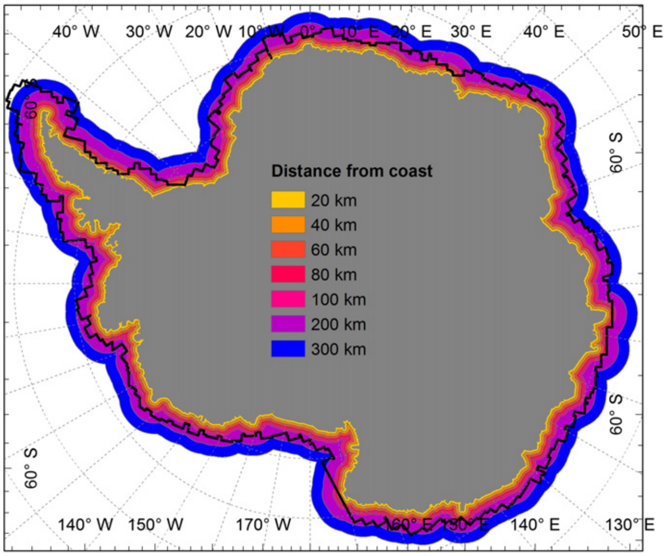

Fig. 1. Width of the ocean zone covered by the RAMP AMM-1 mosaic. The black line shows the edge of the area covered by the SAR images. The colors represent the distance according to the legend. Antarctic coastline is taken from Byrd Polar Research Center (http://bprc.osu.edu/rsl/radarsat/data/).

The radar intensity scattered back from sea ice and icebergs depends on the radar frequency, the incidence and look angle of the radar sensor, the polarizations of the transmitted and received radar waves, and on the physical properties of the ice volume (e.g. density, layering, number and size of air inclusions) and the ice surface (roughness in the centimeter and decimeter range) (e.g. Dierking and Wesche (2014)). Icebergs consist of freshwater ice. In general, the incident radar signal penetrates into the bulk of the iceberg and volume scattering is dominant. Liquid water in the upper layers of the iceberg reduces the penetration depth and hence the volume scattering contribution. Although the surface scattering intensity may increase, because of a larger dielectric contrast between the air and the moist or wet surface, the total backscattering coefficient of the iceberg decreases (Wesche and Dierking, 2012). Small icebergs tend to topple or turn over as reported by Scambos et al. (2009) who investigated disintegration processes at the Wilkins Ice Shelf. If the surface of the iceberg is wet, or marine ice attached at the bottom of the iceberg is turned up, the radar signature of the iceberg changes (Dierking and Wesche, 2014).

Sea ice is a mixture of ice, brine (saline liquid in cells between the ice crystals) and air bubbles. Their relative fractions depend on the age of the ice. Salinity, temperature, and density of the ice affect the dielectric constant and the penetration depth of the radar waves into the ice and thus have a large influence on the radar backscattering (Rees, 2006). The radar intensity of new and first-year sea ice is dominated by surface scattering and relatively low, whereas in case of the older, less saline ice, the volume scattering intensity increases, which reduces the contrast to freshwater ice (Wesche and Dierking, 2012). Sea ice is subjected to drift processes (except for fast ice). Convergent motion may create deformation structures, roughening the surface and changing the local ice volume, leading to complex interaction mechanisms between the radar waves and the ice, and hampering reliable iceberg detections as shown by Wesche and Dierking (2012).

The radar signature of open water depends on the wind conditions. The backscattered intensity increases at larger wind speeds, which means that smaller icebergs may be difficult to identify, or strong reflections from the water surface may be automatically classified as icebergs. The optimal conditions for iceberg detection are low wind speed and freezing conditions or the presence of young saline sea ice without any deformation structures (Wesche and Dierking, 2012).

The automated iceberg detection requires the definition of thresholds of the radar intensity to separate icebergs and sea ice in the SAR image. The thresholds were derived from 281 icebergs (0.3 to 434 km^2 in size) and 23 sea ice areas (each 118 km^2 large). To reduce false detections, we assumed that the detection is reliable only if the target was larger than 30 image pixels (corresponding to an iceberg size of 0.3 km^2). However, we cannot exclude that some of the identified smaller objects were indeed icebergs. After the automated detection, we carried out a visual inspection to increase the quality of the result. Obvious false detections (e.g. sea ice ridges, spots of rough open water) were removed. Missed icebergs or unrecognized portions of larger icebergs were marked as detected. Further details of this procedure are provided below.

In Fig. 2, examples of the detections result are presented for different regions. The Shackleton Ice Shelf is characterized by a large fast ice zone adjacent to the ice shelf (see Fig. 2, panel A) and drifting pack ice A large number of icebergs are captured in the fast ice. One large iceberg, visible on the left, is still located close to the ice shelf (Fig. 2, panels A and B). The Land Glacier region has a complex assemblage of small free drifting icebergs, bergs captured in the fast ice and nascent bergs partially connected to the glacier terminus (Fig. 2, panels C and D). The third region is the ocean region north of the Fimbul Ice Shelf. Compared to the other two regions, there are only a few icebergs visible (Fig. 2E and F).